BULLETIN OF THE POLISH ACADEMY OF SCIENCES
TECHNICAL SCIENCES, Vol. 58, No. 4, 2010
DOI: 10.2478/v10175-010-0048-9

Fibre lasers – conditioning constructional and technological

A. ZAJĄC[1,2*], D. DOROSZ[2], M. KOCHANOWICZ[2], M. SKÓRCZAKOWSKI[1], and J. ŚWIDERSKI[1]

[1], Institute of Optoelectronics, Military University of Technology, 2 Kaliskiego St., 00-908 Warszawa, Poland
[2] Faculty of Electrical Engineering, Bialystok University of Technology, 45d Wiejska St., 15-351 Białystok, Poland

Abstract. In this paper the actual level of fiber lasers' development is presented. There is also presented the analysis of technological and constructional conditions that limit energy parameters of those sources.

Authors also show a construction and a technological work, conducted in Poland, which led to improving energy and exploit parameters of fiber lasers.

Key words: fibre lasers, conditioning constructional, conditioning technological.

1. Introduction

The year of 1960 was a breakthrough in the optical science – on 16th May the first laser was built.

The properties of laser beam – monochromatic, coherent and collimated beam – had not been possible to get in existing sources of optical radiation in visible spectrum until that moment.

All the fifty years from that moment is a history of an effective reaching the coherent beam at gradually higher parameters. The history of lasers is rich in important breakthroughs. One of those instances is projecting in 1961 and building in 1962 by Snitzer a laser of the fiber geometry [1, 2]. The presented construction was only a kind of curiosity for that moment. Besides an unimpressive beginning, the idea of the laser of geometry (and the characteristic of cluster) corresponding with an optical fiber has survived until now. In the last 15 years the idea of fiber laser has come into fruition and such fast development as well as the dynamic growth had not been observed in 50-year history when other lasers are concerned. At the moment the presentation of fiber lasers includes two main groups of technical solutions: microlasers using fiberlasers of geometry corresponding with fibers typical for integrated optics – rectangular (or more complicated – for instance comblike) used in planar structures and, lasers using optical fibers with cylindrical symmetry, typical for telecommunication structures and fiber lasers. The last mentioned are divided in three main groups: fiber lasers and amplifiers used in optical telecommunication with low powers of diode pump (ca 1 W) and low powers of beam. This kind of lasers are pumped into the core with addition of prazeodymian (PDFA) and erbian (EDFA) ions and are pumped longitudinally, which means that in an active core there are simultaneously led: radiation of the pump and a generated radiation – of an optical signal, fiber lasers using up-conversion in the pumping process purposing to generate a laser beam in a visible spectrum and fiber lasers of medium and high power built with double-clad fibers.

Typical, basically known the 1964's configuration of a fiber laser set-up fulfils two basic conditions: an active centre is a core of an optical fiber with addition of rare earth ions (it is likely to use a single-mode fiber but in many applications also a multi-mode fiber is used), an active addition is optically stimulated – for lasers of medium and high power it is effective in the configuration of lateral pumping (distinct from the typical set-up used in fiber telecommunication where the longitudinal pumping is used) with the use of coherent pumping of laser diodes of the power from a few to dozens of Watts (for generating powers from a few to dozens of Watts there are also used set-ups of pumping from the forehead of the fiber, using single semiconductor lasers or set – ups of several single semiconductor lasers set in parallel.

Lasers of medium (up to several Watts) power made in fiber technology, up to the mid-nineties of XX Century did not meet the possibility of practical application. This had not changed until the two factors, changing technological conditions, were invented: development of efficient semiconductor lasers' technology with the emission wavelength adjusted to the absorption band of rare earth ions and development of double-clad fiber perfectly matching the geometry of semiconductor laser beam – open a new chapter in development of fiber lasers. From that moment the two above factors have been developed until now, there is a constant growth of technology of fiber lasers. In Fig. 1 there is a graph showing actual achievements in the field of lasers, made in this kind of configuration.

From 1995 up to now the power gained in fiber lasers set-ups has raised from the level of 5 W to 5 kW (continuous working CW) with the quality of laser beam M = 1 (SM fibers) and up to 50 kW (MM fibers). Development plans presented by IPG Company tell about possibilities of construction of fiber lasers with powers reaching 100 kW in MM CW. To the considerably minor degree there are results got in impulse lasers' set-ups – Fig. 2. Fiber lasers are not the best solution when it comes to the construction of pulse sources.

*e-mail: azajac@wat.edu.pl

It is because of two problems: a volume of an active centre (core) in a laser with the fiber configuration is extremely low, which limits the energy aggregated in the centre (core) and a small size of generated radiation mode easily leads to the destruction of the fiber material.

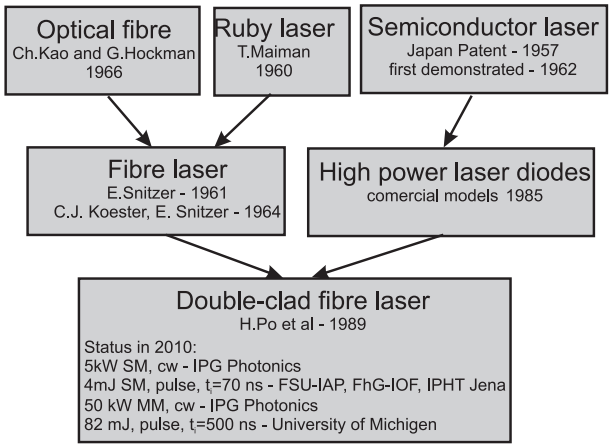

Fig. 1. Milestones of high power fiber lasers

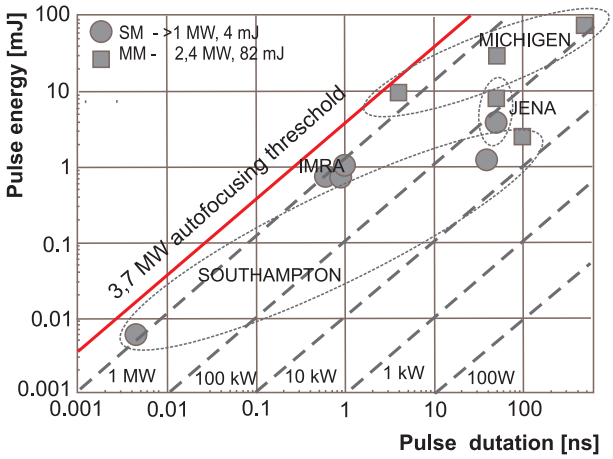

Fig. 2. Energetic parameters of pulse fiber lasers

2. Limitation of parameters of fiber lasers

Considering basic limitations on parameters of laser beam generated in fiber lasers, it is obvious that the essential problems are the destructive mechanisms in SM fibres, determined by nonlinear effects, thermal effects, or – in case of generation of short – nanosecond or subnanosecond pulse duration, field effects (e.g. ionization). All these effects limit the maximum energy parameters of laser beam in the amplifier set-up or a fiber generator. In addition the non-linear effects play an important role. Fiber lasers are sources of radiation with parameters far-distant from the classical SSL.

Typical lengths of optical fibre used for construction of fibre laser are between 0.5 and 50 metres (accordingly photonic fibres for sources of radiation of "super-continuum" type as well as fiber lasers of medium and high power in one-element version). Diameters of the core of active fiber are between 5–50 μm, and, they are depending on the diameter, they have numeric aperture NA between 0.2 and 0.04. These characteristics determine the limitation of possible to reach time parameters of the energetically active beam. In Fig. 3, there is depicted a relationship of the influence of the length of the active core (medium) on the problems of limiting values of energetic parameters of laser beam obtained in DPSSL constructions and fiber lasers. The raising length causes occurring problems connected with nonlinear effects and, at the same time, it limits thermal effects which are dominant in the typical DPSSL lasers.

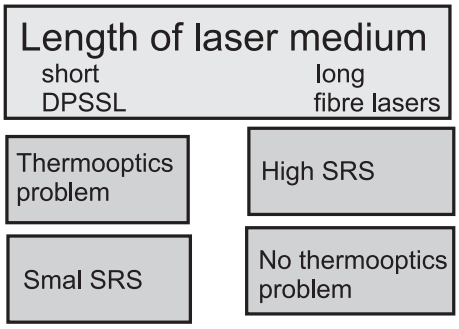

Fig. 3. Optical and thermal properties of fibre laser vs DPSSL

The principal influence on the parameters of the light beam in the fibre lasers of this kind of set-ups have: ASE (Amplified Spontaneous Emission), SRS (Stimulated Raman Scattering), SBS (Stimulated Brillouin Scattering), RBS (Rayleigh backscattering), fiber field or the thermal damage threshold.

2.1. Amplified spontaneous emission. The certain part of the energy aggregated in an active core is lost, during spontaneous emission, beamed out both in the core acceptance angle and outside the core of the fibre. The energy propagates along the fibre together with the pump radiation, it can also go through core area being at the same time reinforced. That is from where the name "amplified spontaneous emission – ASE" comes from. With high levels of amplifying (and those occur in fibres) ASE for the part of emitted radiation led in the core can reach very significant value, minimizing as well inversion of populations in the active medium. It is basically important in case of pulse fibre lasers [3] and pulse amplifiers MOFPA [4–6]. The noise signal (ASE), in given point of fiber, is proportional to the product of the Planck constant, frequency ν, and the width of amplifying band $\Delta\nu$ [5, 6] – $P^0_{ASE} = 2h\nu\Delta\nu$. The ASE signal can propagate in both directions – along and opposite to the direction of pump radiation propagation. There are a few methods of reduction of this disadvantageous effect existing. One of them is doping the inside clad of fiber with non-linear absorber [7], getting with the process inhibiting of the growth of initially weak hub of spontaneous emission. Another solution is, for instance, an immision of narrowband optical fibers fit along the core of the fibers into the set-up [8]. In the case of high power set-ups a good solution (in fact the most commonly used) is the usage of LMA fiber.

2.2. Stimulated Raman Scattering. Quartz is not a strong nonlinear material, but with the influence of radiation of high summit power or density it shows major nonlinearities. These are negative effects and they occur below the threshold of damage of the fiber. One of those effects is Stimulated Raman Scattering. SRS is an effect of interaction of light wave and molecular quartz (SiO_2) vibrations. SRS can occur in both directions (along and opposite to the direction of stimulation wave). The threshold of back scattering is much higher than of collinear scattering and as a rule in fibers only and dispersion in direction along with the direction of stimulation wave propagation. The level of threshold power of *SRS* – P_{SRS} is theoretically assigned and experimentally proved and is described with the relation: $P_{SRS} = 16A_{eff}/L_{eff}g_R$ [9–11]. In the presented relation there is used a concept of the effective fiber length, which differs from the geometrical length l_w because of exponential suppressing of the propagating wave in the optical fiber and it can be found from the relation: $L_{eff} = (1/\alpha_p)\,[1 - \exp(-\alpha_p l_w)]$. The other values mean: g_R – coefficient of Raman amplifying, α_p – coefficient of radiation inside the fibre absorption of elementary length, $A_{eff} = \pi w^2$ – effective surface of the mode field of propagating signal (approximately the core of the fibre); w – diameter of propagating beam in the fibre. Spectrum of Raman amplifying is very wide (ca 30 THz). The maximum of the Raman amplifying is about 1×10^{-13} m/W (for the radiation of the wavelength of 1 μm) and it appears on the (shifted sideband) at about 13 THz [8, 12].

2.3. Stimulated Brillouin Scattering. **S**timulated **B**rillouin **S**cattering SBS is an effect coming from electrostriction phenomenon describing the fibre material, which generates an acoustic, propagating wave, both with stimulating optical wave. It leads to transformation of frequency and reversal of the direction of light wave propagation. The acoustic wave radiating inside the fibre plays the role of diffraction net, neglecting part of the radiation in the opposite direction to this of optical wave propagation. In contrary to SRS, which is effective both along and opposite to the direction of spreading the signal, SBS occurs in optical fibers only in the backwards direction. It minimize the power of the signalling the fiber and there is a strong returning dispersion wave generated moved into the lower frequencies by the value of $\nu_B = 2nV_a/\lambda_s$ [8]. In this relation V_a is a velocity of acoustic wave propagating in the optical fibre. Brillouin's frequency depends on the velocity of the acoustic wale (in the glass 5960 m/s [40]), Optical wavelength λ_s and coefficient of matrix refraction. The threshold power of SBS P_{SBS} can be described with the ralation $P_{SBS} \approx (21A_{eff})/g_B L_{eff}$, where the effective fiber length is described as $L_{eff} = (1/\alpha_p)\,[1 - \exp(-\alpha_p l_w)]$, and g_B is the Brillouin stimulating coefficient [8]. The signal of stimulated Brillouin scattering for the quartz glass occurs on (shifted sideband) for about 10 GHz, and the stimulation peek's maximum is about 6×10^{-11} m/W ($\Delta\nu_B \sim$ 10–40 MHz) [13].

2.4. Self-Phase Modulation. Self-Phase Modulation SPM is a phenomenon caused by the relation of refractive index of the fiber material and the intensity of radiation propagating inside the fiber $n = n_0 + n_n I$. For the silica glass the value of coefficient n_n is between 2.2×10^{-20}–3.4×10^{-20} m^2/W. The radiation pulse in the way l_w in the fiber got the phase delay, related in time to time amplitude, by the value described as relation: $\phi_{NL}(L) = [(2\pi\ n_n\ l_w)/\lambda]\, I$ [14]. A time change of phase delay $\phi_{NL}(L)$ corresponds to the change of the light impulse frequency about the value of $\Delta\nu(t) = \dfrac{2\pi\ n_n\ l_w}{\lambda}\dfrac{dI(t)}{dt}$ [14]. As a consequence the impulse got spectrally widened. This phenomenon can be stronger for propagation inside the fiber with characteristic of normal group dispersion and can be partially reduced by using a fiber with an abnormal dispersion.

2.5. Rayleigh backscattering. In every optical fiber occurs a phenomenon of Rayleigh backscattering. Irregularities of refraction coefficient in micro scale in the glass cause RBS. Rayleigh backscattering is elastic and occurs without the change of energy. It depends mostly on the wavelength of radiation propagating in the optical fiber and does not depend on the intensity of radiation. Losts caused because of RB, for silicon glass, can be described by the relation $\alpha_R = k_R/\lambda$, where k_R is a material coefficient [14]. Losses caused by this phenomenon for the wavelength about 1 μm are between 0.6–1 dB/km.

2.6. Fiber damage threshold. Too big intensity of radiation in the core of the fiber can lead to the damage of its forehead. For pure quartz (SiO_2) the optical damage threshold is about of 50 GW/cm^2 [15]. In case of active silicon glass fibers the threshold is much lower – amounts to about 2–3 GW/cm^2 [16]. A value of the threshold can decline – as a result of a low quality (different kinds of flaws) of the fiber material and in the case of a low precision of polishing the surface of optical fiber's foreheads. The fiber damage threshold can be raised by the usage of fibers with higher diameters of an active core and by using flat – parallel tiles made of materials with the refraction coefficient identical as the material of the fiber core thick of 3–5 mm, welded to the ends of the fibers – so called "end cap".

3. RE ions doped in the active fibers

The development of rare earth doped optical fibres enabled to produce fibre lasers with a very good quality of the radiation beam. The essential role is played here by the double clad active optical fibre, different from the structure of the conventional one. In the classical double clad active fibre it can be collected relatively small amount of energy, mainly because of a thin core (single mode operation) and clustering phenomena. In order to increase RE concentration LMA fibres were developed. The other way to increase active dopant in the optical fibres can be realised in off-set fibres with helical eccentrically located core and multicore optical fibre which are the subject of the research conducted by the authors of this paper.

The active fiber doped of rare earth ions in the lasers and amplifier set-ups are used. Most of the set-up of extreme en-

ergy parameters is made of an active fiber doped of iterbium and doped of neodymian is also still often used. The structure of levels of those two main active rare earth doped is depicted in Fig. 4. The analysis of energy levels set-up shows the reasons for which iterbium is dominating activator in high power set-up – this element has limited spectrum, and that is why there are significantly less problems with the ASE (absorption of excited state). Additionally the absorption band used to stimulating is located very close to the emission band – Stockes efficiency is 92%, with the value of 70% for neodymium. In the last few years in high power laser set-ups new active additions occurred – e.g. erbium, tulium, holmium and their combinations. Basically the possibilities in this range determine technological conditions in production of semiconductor lasers purposed for stimulating of fiber set-ups – typical pump wavelengths (LD generation) are 806 nm (Nd ions stimulation) and 976 nm (Iterbium ion stimulation.

In modern active fibers technology addition of more than one rare earth elements is commonly used, co-doping allows for inclining the absorption efficiency of pump radiation, usage of pumping diodes with available emission bands to pump the addition of absorption band beyond the most efficient emission bands of semiconductor laser, inclining of the total efficiency of laser set-up and, in further perspective, reaching the possibility of usage one addition for pumping another one in one fiber [17–21]. It is not out of the significance that there is also a possibility of developing a generation of high power/energy radiation in the spectrum range between 1400 and 2200 nm. Typical pairs of ions in active fiber co-addition are: Nd^{3+}/Yb^{3+} [21], Er^{3+}/Tm^{3+} [22, 23], Yb^{3+}/Er^{3+} [24], and Tm^{3+}/Ho^{3+} [25]. Pairs used for many years – Nd^{3+}/Yb^{3+} and Yb^{3+}/Er^{3+} – were the solution to the problem of pumping the active addition. In the case of the pair Nd^{3+}/Yb^{3} this combination allowed for reaching a record – 150 W-value of generating power in the laser set-up pumped from the forehead [26]. The pair of ions Yb^{3+}/Er^{3+}, used in set-ups generating in the band of 1500 nm, allows for increasing the pumping efficiency of an active fibre. Using this kind of adding in IPG Company they developed a fibre laser generating of 100W of continuous power in this spectral interval. These kinds of lasers were used as a pump for the 150 W fibre laser, in addition with tulium. In an analogical set-up it was reached 10W tuning range in the spectrum of 50 nm radiation within the spectral range 1700–2000 nm [27].

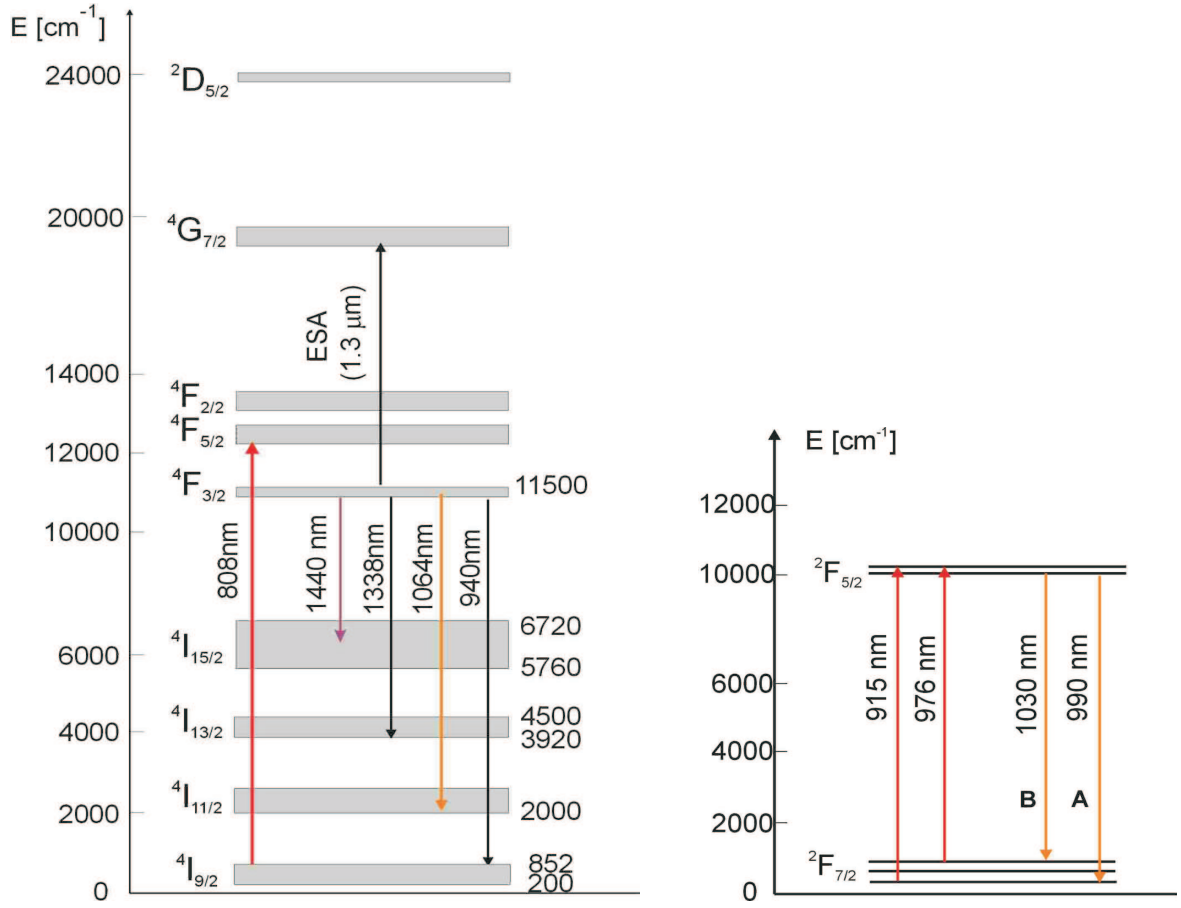

Fig. 4. Structure of energy levels of neodymium ions (left) and ytterbium ions (right)

4. Active fibers geometry

In the fiber laser construction classic fibers (in high power set-ups only double-clad) have a dominating role. Since the last few years there have been intensive works on photonic fibres, and as it seems to be in the perspective of the next few years, the importance of this kind of fibres should incline. In Fig. 5 there are depicted limitations according to used fibres [28, 29].

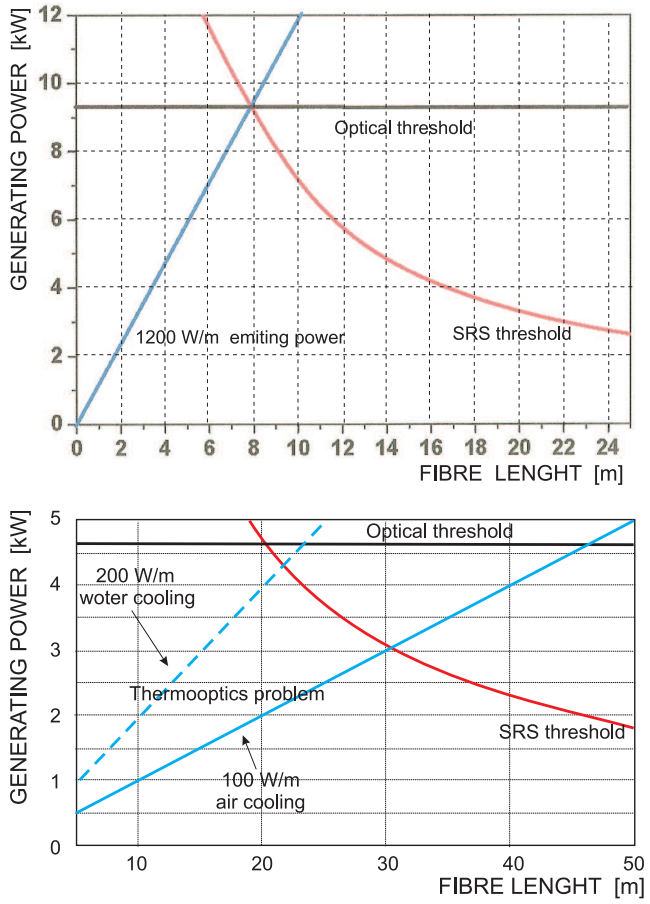

Fig. 5. Limitations of energy parameters in fibre lasers set-ups for clasic double-clad fibre 40 μm core diameter (top) and fotonic fibre 30 μm core diameter (bottom)

As it can be seen the destruction of a threshold and the Stimulated Raman Shuttering – for this diameter is the same, but there are different thermal conditions. This discrepancy is a result of existence of air clad surrounding the auditioning core in the fibre structure – Fig. 6. There is one significant advantage of the photonic fibre – for proper parameters, it always become SM – Fig. 7. This characteristic is important when it comes to wide spectrum generations –e.g. super continuum, and for the impulse set-ups allowing for boosting the power accumulated in the active fibre. The only limitation in usage of the LNA core fibers is loss which occurs when the product d/Λ, is little (below 0.1) [30]. In the last few years one more idea has emerged, increasing the volume of active fibre core (and what is a consequence of increasing the energy accumulated in the active fibre core). The idea is about preparing a double- clad fibre with the cylindrical clad and a helical core [31, 32].

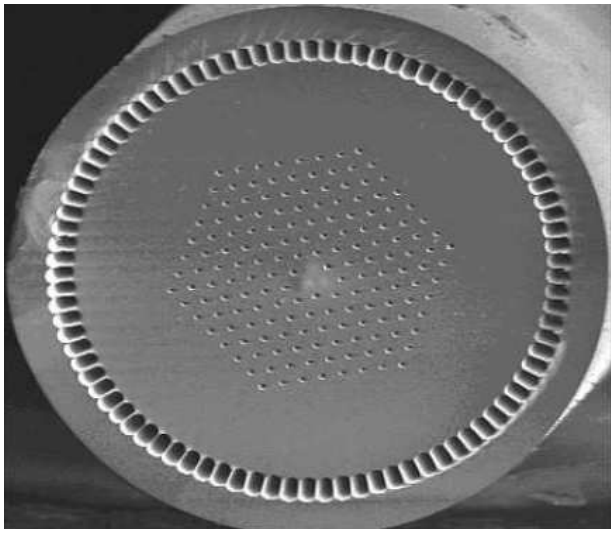

Fig. 6. Cross-section of fotonic fibre

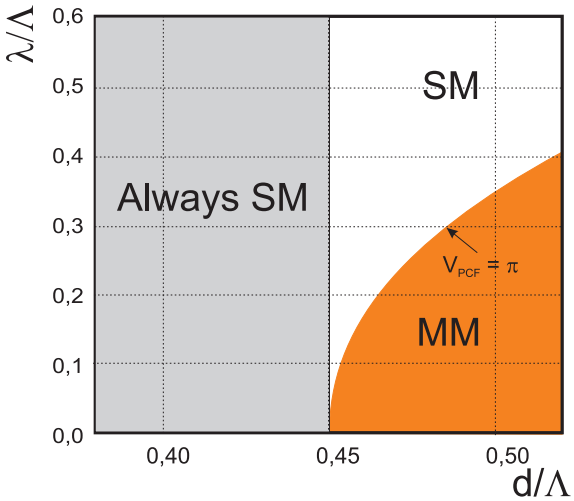

Fig. 7. Classification of fotonic fibre based on modality of structures. In the fotonic fibre set-up for the relation of air channel diameter d to the period of structure Λ lower from 0.45 the fibre is always SM

Because of convolute shape of the fiber core it is possible to get SM distribution of the field with the larger diameter of a core. The schematic fibre is shown in Fig. 8. An additional benefit of this kind of geometry is a possibility of simpler cutting of the fibre (typical cutters are used) and, at the same time in case of using the fibre for construction of the amplifier, this cutting causes detention of the fiber cross-section.

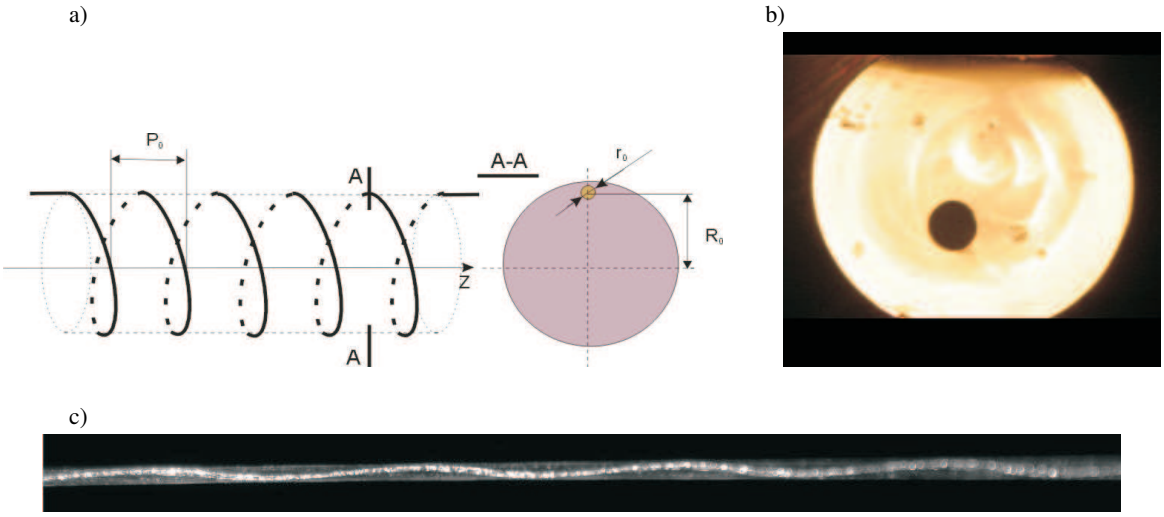

Fig. 8. The idea of double clad helical core fiber a) geometrical scheme of helical core fiber, b) cross section of fiber, c) view of optical fibre

4.1. Helical core optical fibre doped with Nd $^{3+}$/Yb^{3+} ions. Energy transfer between lanthanide ions takes place when absorption, and emission occur in different optical centres. The theoretical description of this phenomenon is based on the examination of interactions appearing between active cores. In consequence of matching the values of the emission cross-section of neodymium $\sigma_{em(Nd)}$ and the absorption cross-section of ytterbium $\sigma_{abs(Yb)}$ in the glass doped with 0.15Nd^{3+}:0.45Yb^{3+} a broad ($\Delta\lambda = 100$ nm) luminescence band in the vicinity of 1 μm was obtained. Its half-intensity width is almost three times larger than in case of the glass doped with neodymium ions [33, 34]. This phenomenon is connected with the non-radiative resonance interaction between rare earth ions. On the basis of absorption and emission spectra in Nd^{3+}/Yb^{3+} doped glasses a diagram of energy levels was created (Fig. 9). While analyzing the energy level structure of the neodymium and ytterbium, the emission spectra is the superposition of the $^4F_{5/2} \rightarrow {}^4I_{9/2}$ (Nd^{3+}) and $^2F_{5/2} \rightarrow {}^2F_{7/2}$ (Yb^{3+}) optical transitions. The luminescence spectra of the manufactured glasses (SiO_2 – PbO – PbF_2 – B_2O_3 – Na_2O – K_2O – Al_2O_3) under excitation of 808 nm laser diode are shown in Fig. 10.

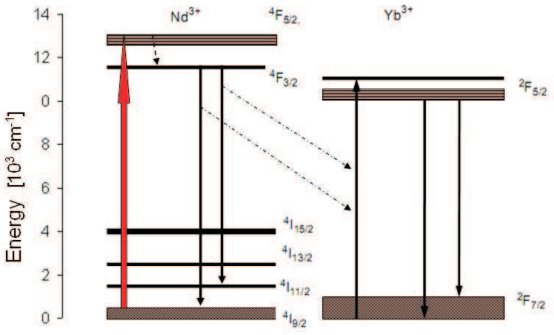

Fig. 9. Simplified energy level diagram with the possible energy transfer mechanism (dotted arrow) in Nd^{3+}/Yb^{3+} co-doped *glasses*

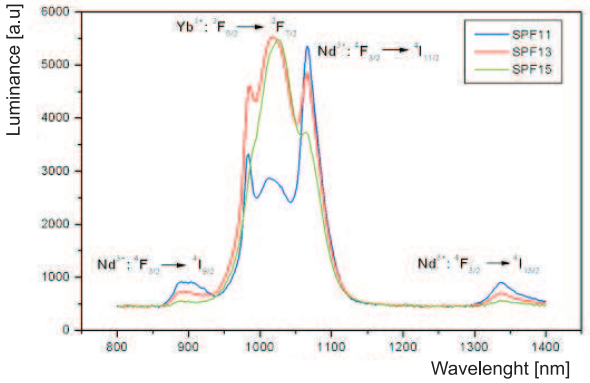

Fig. 10. Luminescence spectra of doped glass with Nd^{3+}/Yb^{3+} (SPF11, SPF13, SPF15) $\lambda_p = 808$ nm

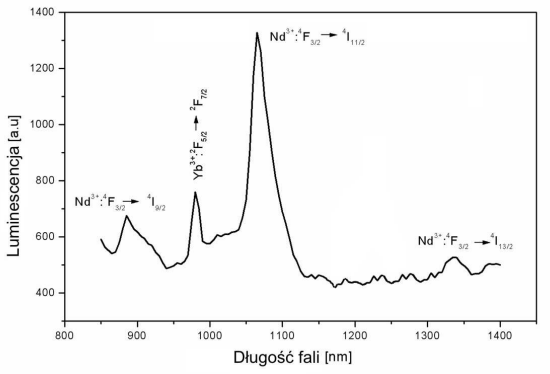

Fig. 11. Cross section (a), and luminescence spectrum (b)of the helical optical fibre, core/cladding diameter – 40 μm/400 μm, pitch of the helix 12.5 mm, core off-set 130 μm, NA-0.127

Glass from the system SiO_2 – PbO – PbF_2 – B_2O_3 – Na_2O – K_2O – Al_2O_3 doped with Nd^{3+}/Yb^{3+} (0.15:0.75 mol%) was used as a core in helical core optical fibre. The authors of this paper achieve the preform by rotating during the technological process. Such a structure of the optical fibre enables to obtain high absorption coefficient of the pumping radiation and larger volume of the core, preserving single mode operation (a helical core forms a mode selector). The cross section and luminescence spectrum of the fibre are presented in Fig. 11.

4.2. Double-clad multicore optical fiber doped with Nd^{3+}. In the double-clad multicore optical fibers the accumulated amount of active dopant ions is significantly greater than in a classical single-core optical fiber. This enables to increase the ability to accumulate energy by the active medium, thus facilitating the N-fold reduction of the fiber length (where N is the number of cores), necessary to absorb the pumping radiation. The basic problem of such a structure is, however, a low quality of the laser beam. The radiation intensity and the beam divergence in such a case are changing proportionally to the number of emitters. If radiation generated in particular cores is mutually coherent (phased), then the far-field diffraction pattern of the laser beam consists of a central high-intensity and low-divergence peak and symmetrical side lobes with considerably lower radiation intensity [35, 36]. The angular divergence of the central peak is reduced in proportion to the number of emitters (elements of the matrix) generating mutually coherent radiation.

Far-field pattern of the active multicore optical fibre. The arrangement of cores in the analysed multi-core optical fibre is shown in Fig. 4. Such a structure has been chosen because of the desired shape of the far-field pattern. Single-mode cores are located in a common cladding. The analysed optical fibre has the following parameters: diameter of the cores $2r = 10$ μm, normalized frequency $V = 2.4$, distance between the cores $d = 10$ μm. The spatial distribution of the emitted laser radiation for each core is described by the Gaussian function. The far field diffraction pattern in the Fraunhofer diffraction region is determined according to Eq. (1) [36, 37].

$$U(x_0, y_0, z_0) = \frac{\exp(ikz)\exp\left[i\dfrac{k}{2z}(x_0^2 + y_0^2)\right]}{i\lambda z} \cdot \iint U(x_1, y_1)\left[\exp(-i(x_0 x_1 + y_0 y_1)\right] dx_1 dy_1, \tag{1}$$

where: $k = 2\pi/\lambda$, λ – wavelength, $(x_0,\ y_0)$ and $(x_1,\ y_1)$ – points coordinates respectively – image plane and $z = 0$ plane.

In the far-field pattern, assuming that the radiation phase in each core is identical, the central peak intensity is much bigger than in the case of free running emitters (Figs. 12 and 13). It should be noted, however, that the laser spot diameter is inversely proportional to the number of cores.

In the presented case, authors analyzed the impact of partial exchange of the radiation generated in the fiber cores on the phase difference between particular emitters during development of the laser action in the fiber laser constructed on the basis of the 5-core optical fiber described above.

a)

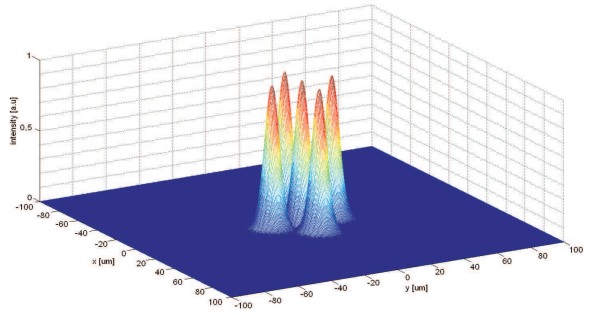

b)

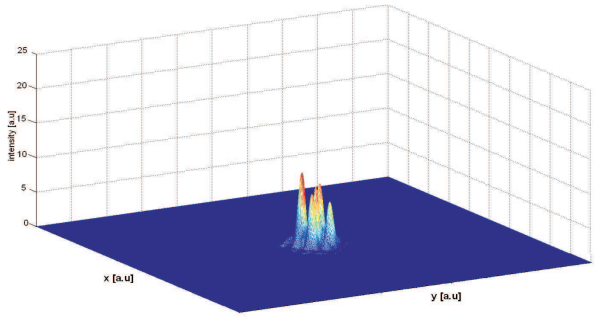

Fig. 12. Near field pattern (a) Far field pattern (b) of 5 – core optical fibre, $V = 2,4$ $2r = 10$ μm, random phases

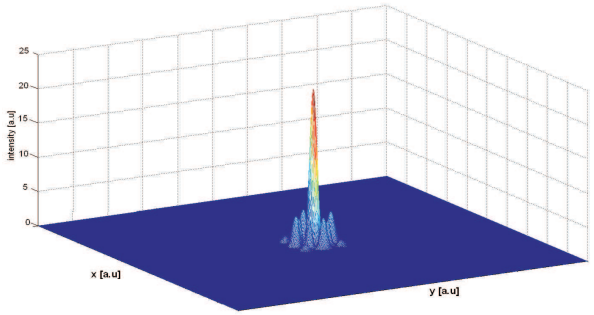

Fig. 13. Far field pattern of 5 – core phase - locked optical fibre, $V = 2,4$ $2r = 10$ μm

Along with the rise in the number of passages of the photon flux through resonator, the phase angle in each core approaches the value of the radiation phase in the second core (Fig. 14). For example, after 100 passages through a resonator with the coupling coefficient changing within the range $C = 5$–10%, the phase difference between radiation in particular emitters approximates zero. In the analyzed fiber laser the exchange of min. 5% of the radiation generated between adjacent cores on the fiber length ($L = 5$ m) results the radiation in the five cores is phase - locked. Then, the field distribution in the Fraunhofer diffraction region takes the shape shown in Fig. 15.

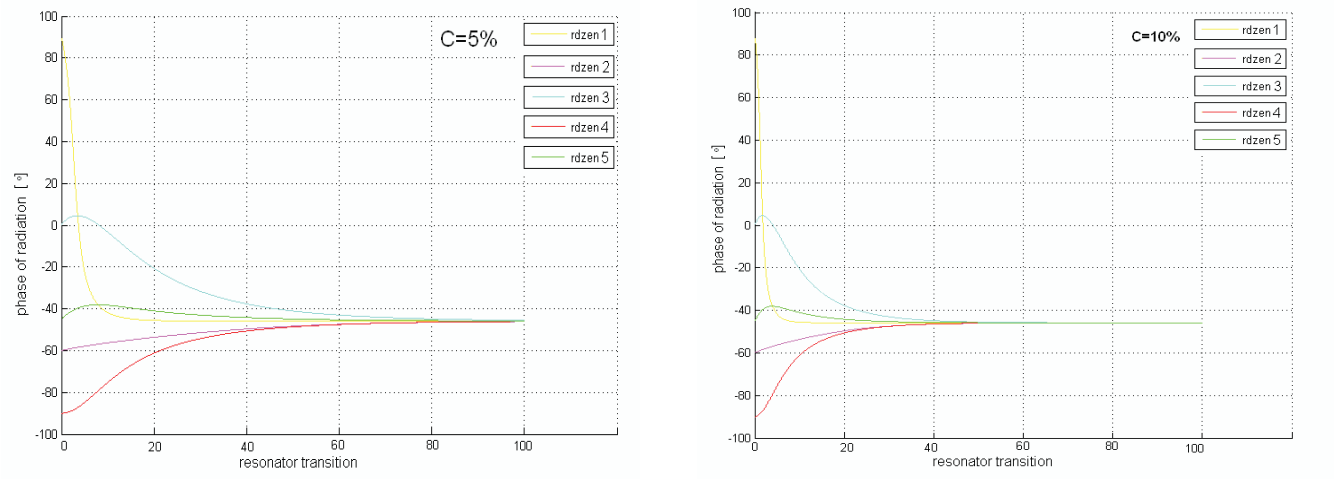

Fig. 14. Radiation phase changes in cores vs number of fiber laser resonator transitions for $C = 5$ (a), $C = 10\%$ (b)

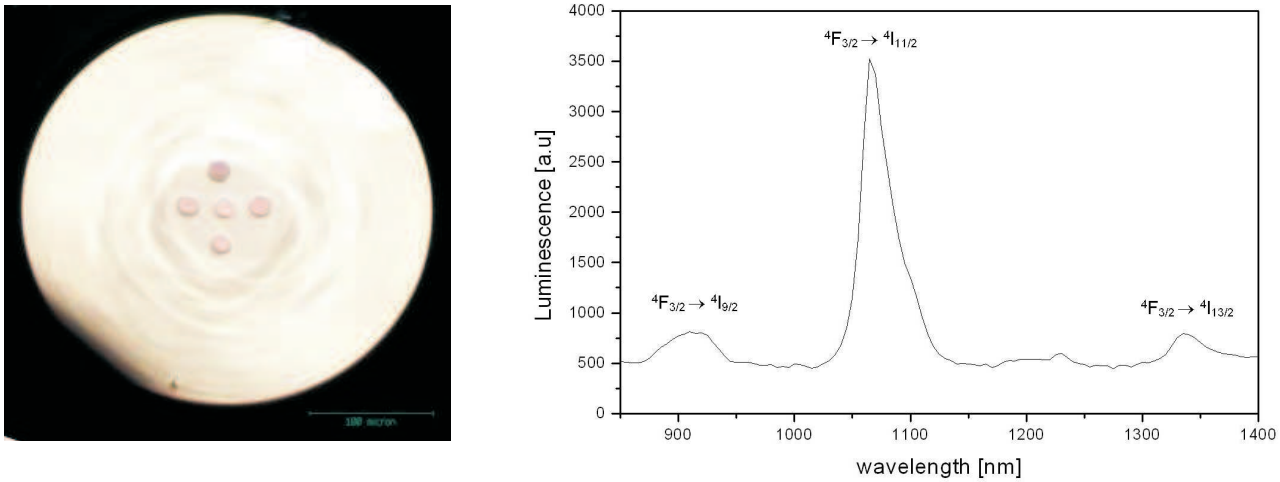

Fig. 15. Cross section (left) and luminescence spectra (right) of the fabricated multicore fibre

Fig. 16. Cross-section of tellurite optical fibre moped with Yb^{3+}/Tm^{3+} (1:0.1 mol%), core/cladding diameter 40μm/450μm

The large numerical aperture diameter of inner cladding and numerical aperture ($NA_{\text{inner cladding}} = 0.58$) enables effective coupling of the pump laser diode with the obtained fibre. The luminescence spectra of the manufactured multicore fibre under excitation through inner cladding by the laser diode AlGaAs ($\lambda = 808$ nm) are shown in Fig. 16. Emission bands at 900 nm ($^4F_{3/2} \rightarrow ^4I_{9/2}$), 1060 nm ($^4F_{3/2} \rightarrow ^4I_{11/2}$) and 1330 nm ($^4F_{3/2} \rightarrow ^4I_{13/2}$) were attained. Due to the four-level quantum scheme operation the optical transition ($^4F_{3/2} \rightarrow ^4I_{11/2}$) related with luminescence band at 1060 nm is the most efficient. However, emission at 900 nm and 1330 nm, usually unparalleled in silicate glasses were also observable.

4.3. Up-conversion luminescence in tellurite optical fibre. Figure 16 presents an optical fibre with the core made of tellurite glass (TeO_2 – GeO_2 – PbO – PbF_2 – BaO – Nb_2O_5 – LaF_3) codoped with Yb^{3+}/Tm^{3+} (1:0.1 mol%) ions.

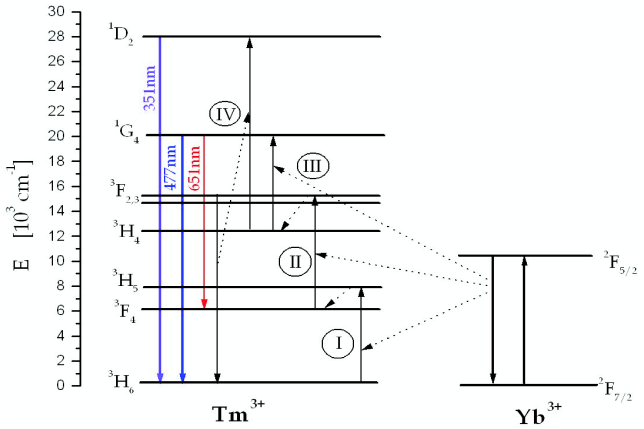

Fig. 17. Simplified energy level diagram with energy transfer in Yb^{3+}/Tm^{3+} co-doped tellurite fibre

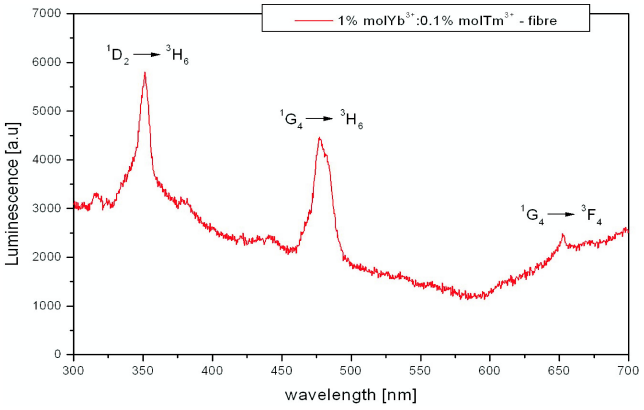

Fig. 18. Luminescense spectra of tellurite doped fibre with 1%molYb^{3+}:0.1%mol Tm^{3+}

The non-resonant energy transfer between Yb^{3+} and Tm^{3+} have been characterized in the tellurite active fibre. Due to high quantum efficiency (∼90%) and wide range of the excitation level, Yb^{3+} (sensitizer) ions are used in co-doped systems to enhance efficiency of luminescence [38]. Figure 17 presents simplified energy level structure with upconversion mechanism. In result of three-photons absorption process and cross-relaxation energy transfer the strong blue emission at 477 nm and ultraviolet emission at 351 nm corresponding to the transitions $^1G_4 \rightarrow {}^3H_6$ and $^1D_2 \rightarrow {}^3H_6$ were observed. The upconversion luminescence spectra in tellurite optical fibre under 980 nm diode laser excitation was measured (Fig. 18). The dependence of the up-conversion emission intensity upon the thulium ions concentration was analyzed. The most effective energy transfer $Yb^{3+} \rightarrow Tm^{3+}$ occurs in the optical fibre with the molar ratio of dopant 1 Yb^{3+} : 0.1 Tm^{3+}.

5. Selected laser systems

In the IOE MUT there was a research of pulse fiber laser set-ups in two configurations – MOFPA and SWEEP LASER. The results of these studies are presented in the following paragraphs.

5.1. Sweep laser. The experimental setup of a sweep fibre laser is illustrated in Fig. 19a. The laser was based on the polarization maintaining double clad Yb doped silica fiber (20 μm core and 400 μm clad diameter) which was pumped by the 976 nm diode laser. The pump radiation was delivered by the Y-type fibre coupler which gives the active fibre caps free and easy coupled with the free-space optics. To tune the laser wavelength the acoustic-optical birefringent tunable filter was used. The diffraction efficiency of the filter was up to 80% and the diffracted beam was used in the feedback branch of the laser. The non diffracted beam was the output of the laser.

The laser was able to work in CW regime but its main mode of operation was the pulsed sweeping. The idea of that operating mode is presented in Fig. 19b. The narrow spectrum loss deep is swept across the laser spectral gain profile in a pulsed way. In practice it was realized by the electrically steered controller which generated the 32 steps voltage signal. Each voltage step was related to a certain value of the wavelength transmitted by the acoustic-optical filter.

The results of the sweep laser generation indicate that the line broadening in the Yb doped fibre is more of homogeneous character then the inhomogeneous one. It is visualized in Figs. 19c and 19d. where the laser action dynamics together with the sweeping voltage are shown. The output of the laser presents only a single pulse, appeared at one wavelength whereas, it should be the train of pulses at different wavelengths if the line was inhomogenously broadened. Some results on the numerical modelling of the laser action in the cases of the both types of line broadening are presented in Fig. 19e (the dynamics of laser action – pink, gain – blue, steering voltage – green).

5.2. MOFPA laser set. In the set-up, as in Fig. 20, there is a possibility of nanosecond time range of laser beam with the usage of a semiconductor laser diode in the role of master oscillator. The presented set-up consists of the master oscillator and the two element cascade of a power amplifier. LD master oscillator emits the laser beam of the wavelength of 1064 nm with a variable pulse time duration within the range of 8.5–250 ns and the repetition range up to 0.5 MHz. The first

amplifier is made of the Yb doped double clad active fiber with the core diameter of 8 μm, and 0.11 NA with the inner clad dimensions of 180×240 μm^2 (rectangular) and 0.45 NA. The semiconductor pump using power of 45W @976 nm was applied. The second amplifier is made of the active of Yb doped double clad LMA active fiber with the core diameter of 20 μm, and 0.06 NA with the inner clad dimensions of 400 μm (octagonal geometry). The semiconductor pump using power of up to 45 W 2976 nm was applied.

The results are presented in Table 1 [39].

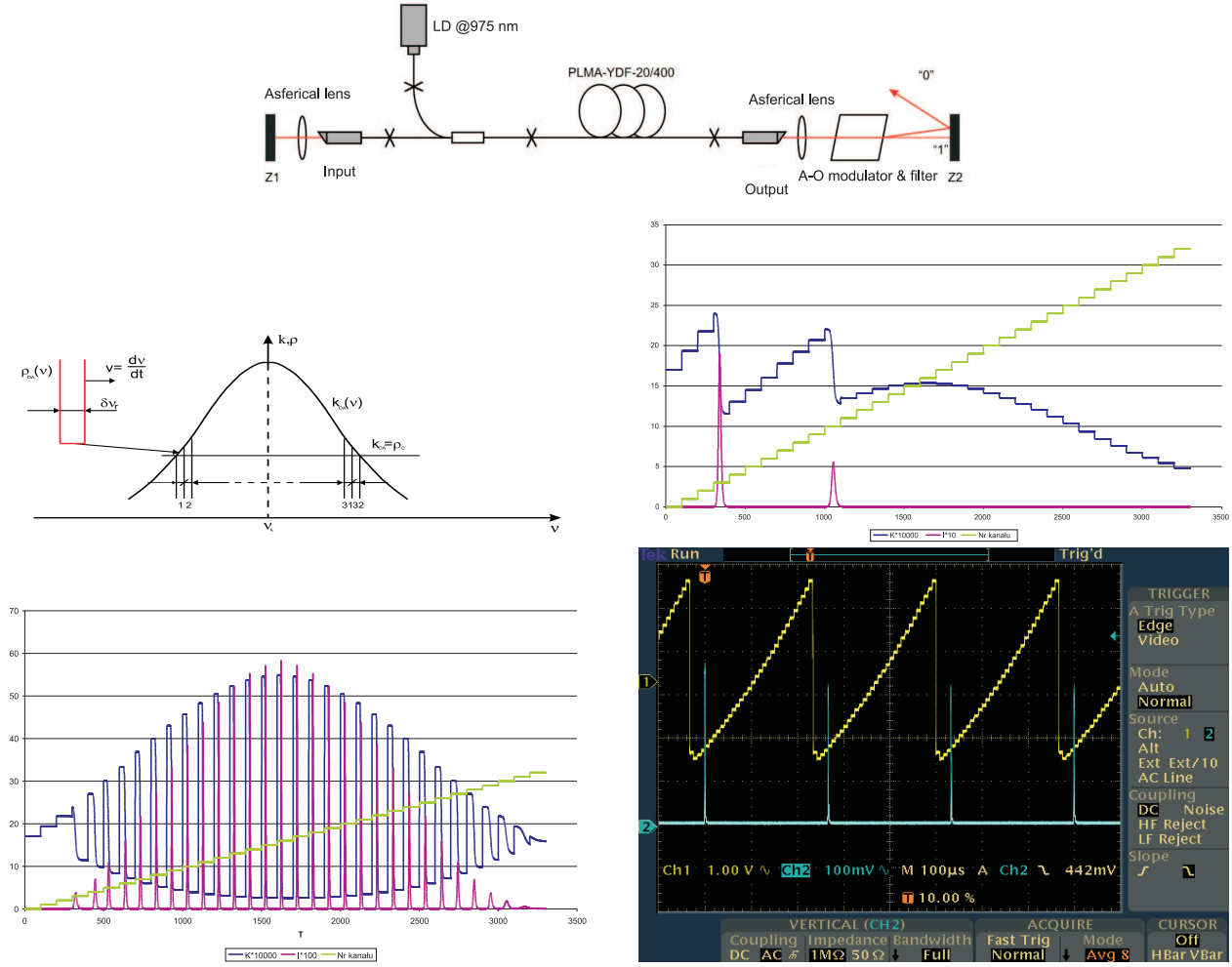

Fig. 19. Optical scheme sweep laser set-up (a), procedures of verification of a sweep laser idea, c) and d) results on the numerical modeling of the laser action in the cases of the both types of line broadening homogeneous (c) and inhomogeneous (d), e) results of the sweep laser generation

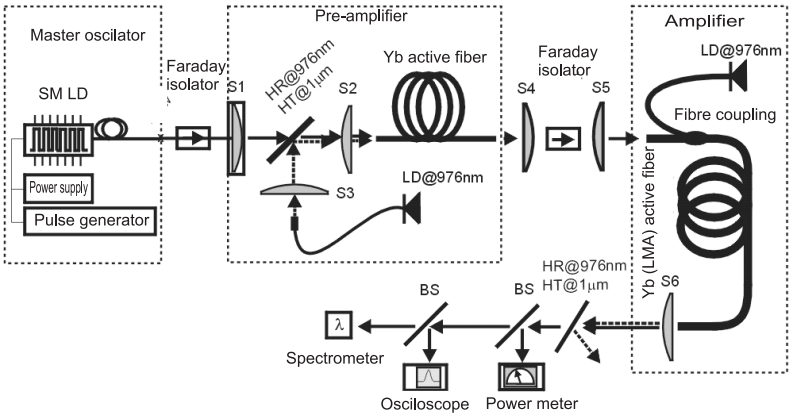

Fig. 20. MOFPA laser set – master oscillator is a special semiconductor LD

Table 1
Time and energetic parameters of laser beam got in the set up showed in Fig. 20 (pump power 37.6 W)

Time duration [ns]	Energetic properties [W]	Repetition rate		
		500 kHz	100 kHz	50 kHZ
250	P_{aver}	22.01	20.9	19
	P_{pulse}	176.08	836	1520
100	P_{aver}	21.30	20.45	18.4
	P_{pulse}	426	2 045	8 680
50	P_{aver}	20.63	19.98	17.82
	P_{pulse}	825.2	3 396	7 128
20	P_{aver}	20.40	–	–
	P_{pulse}	2 040	–	–
8,5	P_{aver}	20.14	–	–
	P_{pulse}	4 739	–	–

6. Conclusions

The fiber lasers (both cw and pulse) are now the modern laser systems allowing for implementation of laser sources in most tasks, in medicine, industry and metrology. The optical and generated energy parameters are characterized by a very high efficiency and the optical quality of laser beam ($M^2 \approx 1$) which create these sources as a leading group of high power laser systems in the very beginning of XXI century.

REFERENCES

[1] E. Snitzer, "Proposed fibre cavities for optical masers", *J. Appl. Phys.* 32, 36–39 (1961).

[2] E. Snitzer, "Optical maser action of Nd^{3+} in a barium crown glass", *Phys. Rev. Lett.* 7, 444–446 (1961).

[3] P. Myslinski, J. Chrostowski, J.A. Koningstein, and J.R. Simpson, "High-power Q-switched erbium doped fiber laser", *IEEE J. Quantum Electron*. 28, 371–377 (1992).

[4] J. Limpert, S. Hofer, A. Liem, H. Zellmer, A. Tunnermann, S. Knoke, and H. Voeleckel, "100-W average-power, high-energy nanosecond fiber amplifier", *Appl. Phys.* B 75, 477–479 (2002).

[5] P.C. Becker, N.A. Olson, and J.R. Simpson, *Erbium-doped Fiber Amplifiers: Fundamentals and Technology*, Academic Press, Boston, 1999.

[6] L. Zenteno, "High-power double-clad fiber lasers", *IEEE J. Lightwave Technol*. 11, 1435–1446 (1993).

[7] G. Larose, A. Chandonnet, and G. Lessard, "Actively Q-switched fiber laser with ASE limiting saturable absorber", *Proc. Int. Conf. on Lasers* 1, 197–202 (1995).

[8] A. Bajarklev, *Optical Fiber Amplifiers: Design and System Applications*, Artech House, Boston, 1993.

[9] H.R. Stolen, "Nonlinearity in fiber transmission", *Proc IEEE* 68, 1232–1236 (1980).

[10] G.P. Agrawal, *Nonlinear Fiber Optics*, Academic Press, San Diego, 2001.

[11] R.G. Smith, "Optical power handling capacity of low loss optical fibers as determined by stimulated Raman and Brillouin scattering", *Appl. Opt*. 11, 2489–2494 (1972).

[12] H.R. Stolen, J.P. Gordon, W.J. Tomlinson, and H.A. Haus, "Raman response function of silica-core fibers", *J. Opt. Soc. Am.* B 6, 1159–1166 (1989).

[13] D.. Cotter, "Stimulated Brillouin scattering in monomode optical fiber", *Opt. Commun*. 4, 10–19 (1983).

[14] M.J. Weber, *Handbook of Laser Science and Technology*, *Optical Materials,* vol. 3, Part 1, CRC Press, Boca Raton, 1986.

[15] A. Tunnermann, "Status and perspectives of fiber lasers and amplifiers", *Proc. Conf. on Lasers and Electro-Optics CLEO* PL1-1-MON, CD-ROM (2005).

[16] Y.A. Barannikov, A.I. Oussov, F.V. Shcherbina, R.I. Yagodkin, V.P. Gapontsev, and N.S. Platonov, "250W, single-mode, CW, linearly-polarized fiber source in Yb wavelength range", *Proc. Conf.on Lasers and Electro-Optics CLEO* CMS3, CD-ROM (2004).

[17] G. Rustad and K. Stenersen, "Modeling of laser-pumped Tm and Ho lasers accounting for upconversion and ground-state depletion", *IEEE J. Quantum Electronics* 32 (9), 1645–1656 (1996).

[18] E. Yahel, O. Hess, and A.A. Hardy, "Modeling and optimalization of high-power Nd^{3+}-Yb^{3+} codoped fiber lasers", *J. Lightwave Technology* 24 (3), 1601–1607 (2006).

[19] A. Tunnerman, *Status and Perspectives of Fiber Lasers and Amplifiers*, Cleo Europe, London, 2005.

[20] P.C. Becker, N.A. Olson, and J.R. Simpson, *Erbium-doped Fiber Amplifiers: Fundamentals and Technology*, Academic Press, Boston, 1999

[21] J. Limpert, "150 W Nd^{3+}:Yb^{3+} codoped fiber laser at 1,1 μm", *Proc. Conf. Lasers and Electronics* 1, 590–591 (2002).

[22] Y.G. Choi, K.H. Kim, B. Joo Lee, Y.B. Shin, Y.S. Kim, and J. Heo, "Emission properties of the Er3+: 4I11/2 → 4I13/2 transition in Er3+- and Er3+/Tm3+ - doped Ge-Ga-As-S glasses", *Elsevier J. Non-Crystalline Solids* 19, 278 (2000).

[23] H. Jeong, K. Oh, S.R. Han, and T.F. Morse, "Characterization of broadband amplified spontaneous emission from an Er^{3+}–Tm^{3+} co-doped silica fiber", *Elsevier Chemical Physics Letters* 367, 507–509 (2003).

[24] H. Sun, C. Yu, G. Zhou, Z. Duan, M. Liao, J. Zhang, L. Hu, and Z. Jiang, "Up-conversion luminescence analysis in ytterbium-sensitized erbium-doped oxide-halide tellurite and germanate-niobic-lead glasses", *Elsevier Spectrochimica Acta* A 62, 1000–1003 (2005).

[25] http://www.photonics.com/content/spectra/2007/October/research/89210.aspx.

[26] V. Dominic, S. Mac Cormack, R.Waarts, S.Sanders, S.Bicnese, R.Dohle, E.Wolak, P.S.Yeh, and E.Zucker, "150W Fiber laser", *CLEO Eur. Conf.* 1, CD-ROM (2004).

[27] www.ipgphotonics.com/products_2micron_lasers_cw_tlr-series.htm.

[28] J. Limpert, A. Liem, M. Reich, T. Schreiber, S. Nolte, H. Zelmer, A. Tunnermqann, J. Broeng, A. Peterson, and C. Jakobsen, "Low-nonlinearity single-transverse-mode ytterbium-doped photonic crystal fiber amplifier", *Opt. Express* 12, 1313–1319 (2004).

[29] E. Shcherbakov, "New achievements in development of superpower industrial fiber lasers and their applications", *Proc. Conf. on Lasers and Electro-Optics* TFII2-3-WED, CD-ROM (2005).

[30] J. Limpert, A. Liem, T. Schreiber, H. Zellmer, and A. Tunnermann, "Power and energy scaling of fiber laser systems based on ytterbium-doped large-mode-area fibers", *Advances in Fiber Lasers, Proc. SPIE* 4974, 135–147 (2003).

[31] P. Wang, L.J. Cooper, R.B. Williams, J.K. Sahu, and W.A. Clarkson, "Helical-core ytterbium-doped fibre laser", *Electronics Letters* 21, 1325–1326 (2004).

[32] Z. Jiang and J.R. Marciante, "Mode-area scaling of helical-core dual-clad fiber laser and amplifiers", *Conf. on Laser & Electro-Optics* 1, CD-ROM (2005).

[33] L.Feng, Q. Tang, L. Liang, J. Wang, H. Liang, and Q. Su, "Optical transitions and up-conversion emission of Tm^{3+-}singly doped and Tm^{3+}/Yb^{3+-}codoped oxyfluoride glasses", *J. Alloys and Compounds* 436, 272–277 (2007).

[34] S. González-Pérez, I.R. Martín, F. Rivera-López, and F. Lahoz, "Temperature dependence of $Nd^{3+} \rightarrow Yb^{3+}$ energy transfer processes in co-doped oxyfluoride glass ceramics", *J. Non-Cryst. Solids* 353, 1951–1955 (2007).

[35] A. Desfarges-Berthelemot, V. Kermene, D. Sabourdy, J. Boullet, P. Roy, J. Lhermite, and A. Barthélémy, "Coherent combining of fiber lasers", *C. R. Physique* 7, 244–253 (2006).

[36] Z. Chen, J. Hou, P. Zhou, and Z. Jiang, "Mutual injection-locking and coherent combining of two individual fiber lasers", *IEEE J. Quantum Electronics* 44 (6), 515–519 (2008).

[37] M. Kochanowicz, D. Dorosz, and J. Żmojda, "Coherent beam combining of active multicore optical fiber", *Proc of SPIE* 750, CD-ROM (2009).

[38] H. Jeong, K. Oh, S.R. Han, and T.F. Morse, "Characterization of broadband amplified spontaneous emission from an Er^{3+}–Tm^{3+} co-doped silica fiber", *Elsevier Chemical Physics Letters* 367, 507 (2003).

[39] J. Świderski, M. Skórczakowski, A. Zając, and S. Kowalczyk, "Two cascade optical waveguide system of MOPFA type generating pulses of variable duration at the repetition frequency within the range of 50–500 kHz", *Messages* 9STL, CD-ROM (2009), (in Polish).